

The correlation between the total magnetic flux and the total jet power

Nokhrina Elena *

*Relativistic Astrophysics Laboratory: Basic and Applied Studies of Space Objects,
Moscow Institute of Physics and Technology, School of Fundamental and Applied
Physics, Dolgoprudny, Russia*

Correspondence*:

Institutsky per. 9, Dolgoprudny, 141700, Russia
nokhrina@phystech.edu

ABSTRACT

Magnetic field threading a black hole ergosphere is believed to play the key role in both driving the powerful relativistic jets observed in active galactic nuclei and extracting the rotational energy from a black hole via Blandford-Znajek process. The magnitude of magnetic field and the magnetic flux in the vicinity of a central black hole is predicted by theoretical models. On the other hand, the magnetic field in a jet can be estimated through measurements of either the core shift effect or the brightness temperature. In both cases the obtained magnetic field is in the radiating domain, so its direct application to the calculation of the magnetic flux needs some theoretical assumptions. In this paper we address the issue of estimating the magnetic flux contained in a jet using the measurements of a core shift effect and of a brightness temperature for the jets, directed almost at the observer. The accurate account for the jet transversal structure allow us to express the magnetic flux through the observed values and an unknown rotation rate of magnetic surfaces. If we assume the sources are in a magnetically arrested disk state, the lower limit for the rotation rate can be obtained. On the other hand, the flux estimate may be tested against the total jet power predicted by the electromagnetic energy extraction model. The resultant expression for power depends logarithmically weakly on an unknown rotation rate. We show that the total jet power estimated through the magnetic flux is in good agreement with the observed power. We also obtain the extremely slow rotation rates, which may be an indication that the majority of the sources considered are not in the magnetically arrested disk state.

Keywords: active galaxies, jets, BL Lacertae objects, non-thermal radiation, magnetic flux

1 INTRODUCTION

One of the key issues of theoretical modeling of relativistic jets is determining the magnetic field magnitude. There are several theoretical ways to estimate the latter. The Eddington magnetic field (Beskin, 2010) sets up an upper limit on the magnetic field magnitude in the vicinity of a black hole, since it is set by equipartition of magnetic field density and the total energy density in the accreting plasma that is needed to support the Eddington luminosity. The state of magnetically arrested disk (MAD) (Narayan et al., 2003; Tchekhovskoy et al., 2011; McKinney et al., 2012) sets up the limiting magnetic field that can be accreted

onto a black hole basing on an assumption that in such a state the pressure of previously accreted magnetic field can affect the dynamical process of accretion itself.

There are observational means to evaluate the magnetic field in a jet. Blazar spectrum is successfully modeled by the synchrotron self-Compton model. The lower part of the spectrum is dominated by synchrotron radiation of relativistic plasma in a jet magnetic field. Thus, the high-resolution radio interferometry observations provide us with data for unveiling the physical conditions at the very jet origin — in so called radio core. The way to estimate the magnetic field amplitude through the observations is measurements of core shift effect together with several theoretical assumptions on the radiating volume properties (Lobanov, 1998). However, the measurement of radio flux itself, or, equally, the brightness temperature, can provide us with the instrument to probe the magnetic field magnitude (Zdziarski et al., 2015; Nokhrina, 2017).

The magnetic field estimates is an important parameter that allows to test the theoretical models against observations. Zamaninasab et al. (2014) used the magnetic field measurements to calculate the flux and to show that the total flux is in accordance with the magnetically arrested state of the sources. In this paper we make use of the brightness temperature and core shift measurements coupled with the transversal jet model to express the magnetic field magnitude and the magnetic flux contained in a blazar jet through the rotation rate of magnetic surfaces. Our aim is to compare the magnetic flux in a jet against theoretically limited flux by MAD state and to estimate the rotation rate. We also test the obtained magnetic flux against the observed jet power. If the jet power P_Ψ is fully determined by the electromagnetic energy extraction mechanism, so we denote it with the subscript Ψ , than it can be expressed as (Beskin, 2010)

$$P_\Psi = \left(\frac{\Psi a}{\pi r_g} \right)^2 c, \quad (1)$$

where Ψ is the total magnetic flux, r_g is a gravitational radius, c is a speed of light, and the rotation rate $a = r_g/R_L$ is a ratio of a gravitational radius to the light cylinder radius R_L .

Although there are estimates for magnetic field amplitude (Lobanov, 1998; Hirokani, 2005; O'Sullivan and Gabuzda, 2009; Nokhrina et al., 2015; Zdziarski et al., 2015; Nokhrina, 2017), it cannot be explicitly used for flux calculation. Indeed, the magneto hydrodynamical theoretical and numerical modeling (see e.g. Lyubarsky (2009); Bromberg and Tchekhovskoy (2016); Nokhrina et al. (2015)) show that the toroidal magnetic field is greater than the poloidal one outside the light cylinder radius. Thus, measurements provide us with the magnitude of the toroidal magnetic field, while the poloidal one is needed to estimate the total magnetic flux (Zamaninasab et al., 2014).

2 MAGNETIC FLUX IN A JET

The observed flux, or observed brightness temperature, can be used to estimate the magnetic field in the radiating domain, and, thus, the magnetic flux. The blazar spectrum in radio band is accurately modeled within the self-absorbed synchrotron model (see e.g. Abdo et al. (2011)). The simplest model for the source is a uniform sphere with chaotic magnetic field B and relativistic electrons with the power-law energy distribution described by the amplitude particle number density k_e and spectral index p :

$$dn(\gamma) = k_e \gamma^{-p} d\gamma, \quad (2)$$

$\gamma \in [\gamma_{\min}, \gamma_{\max}]$ (Gould, 1979), where γ is a Lorentz factor of relativistic plasma. The observed spectral flux S_ν at the frequency ν for the optically thick uniform self-absorbed source of radius R at the distance d can be written using the spectral photon emission rate ρ_ν and effective absorption coefficient \mathfrak{a}_ν as:

$$S_\nu = \pi \hbar \nu \frac{\rho_\nu}{\mathfrak{a}_\nu} \frac{R^2}{d^2} u(2R\mathfrak{a}_\nu), \quad (3)$$

and the function of the optical depth $u(2R\mathfrak{a}_\nu)$ is defined by Gould (1979). The emission and absorption coefficients for the self-absorbed synchrotron model ρ_ν and \mathfrak{a}_ν are the functions of the magnetic field B and of particle number density amplitude k_e . These coefficients, written in a jet frame, i.e. in a frame where the electric field vanishes, are:

$$\rho_\nu = 4\pi \left(\frac{3}{2}\right)^{(p-1)/2} a(p) \alpha k_e \left(\frac{\nu_B}{\nu}\right)^{(p+1)/2}, \quad (4)$$

$$\mathfrak{a}_\nu = c(p) r_0^2 k_e \left(\frac{\nu_0}{\nu}\right) \left(\frac{\nu_B}{\nu}\right)^{(p+2)/2}. \quad (5)$$

Here $\nu_B = eB/mc$ is a gyrofrequency in the jet frame, \hbar is the Planck constant, $\alpha = e^2/\hbar c$ is the fine structure constant, and the functions $a(p)$ and $c(p)$ of the electron distribution spectral index p are defined in (Gould, 1979). The spectral flux depends on the magnetic field amplitude, while the particle number density amplitude defines the maximum of a function u and, thus, the position of the observed radio core — the domain where the optical depth τ is equal to unity. So, the spectral flux measurement provide us with an instrument to evaluate the magnetic field in a source. The spectral flux may be expressed through the brightness temperature T_b as

$$S_\nu = \frac{2\pi\nu^2\theta^2}{c^2} k_B T_b, \quad (6)$$

where θ is the angular size of a radiating domain. Thus one can express the magnetic field amplitude in a source having measured brightness temperature. The method was first applied by (Zdziarski et al., 2015) to check the magnetic field amplitude in AGN radio cores independently of the equipartition assumption. Equating the right-hand sides of equations (6) and (3), and expressing the jet frame values through the nucleus frame values, we obtain for $p = 2$ the magnetic field (Zdziarski et al. (2015), see also details in Nokhrina (2017))

$$\left(\frac{B_{\text{uni}}}{\text{G}}\right) = 7.4 \cdot 10^{-4} \frac{\Gamma\delta}{1+z} \left(\frac{\nu_{\text{obs}}}{\text{GHz}}\right) \left(\frac{T_{b,\text{obs}}}{10^{12}\text{K}}\right)^{-2}. \quad (7)$$

Here Γ is a flow bulk Lorentz factor, z is a source redshift, and δ is a Doppler factor.

On the other hand, the measurements of core shift effect (Lobanov, 1998; Hirovani, 2005; O'Sullivan and Gabuzda, 2009; Zamaninasab et al., 2014) provides the following expression for the magnetic field amplitude B_{cs} at 1 pc distance from the central source:

$$\left(\frac{B_{\text{cs}}}{\text{G}}\right) = 0.17 \left(\frac{\eta_{\text{cs}}}{\text{mas GHz}}\right)^{0.75} \left(\frac{D_L}{\text{Gpc}}\right)^{0.75} \frac{\Gamma}{\chi^{0.25}(1+z)^{0.75} \sin^{0.5} \varphi \delta^{0.5}}, \quad (8)$$

here η_{cs} is a coefficient determining the slope of the apparent core position dependence on the inverse observation frequency:

$$\left(\frac{\Delta r}{\text{mas}}\right) = \left(\frac{\eta_{\text{cs}}}{\text{mas GHz}}\right) \left(\frac{\nu_{\text{obs}}}{\text{GHz}}\right)^{-1}. \quad (9)$$

χ is the jet opening angle that may be obtained having the measured in (Pushkarev et al., 2009) apparent opening angle χ_{app} as $\chi = \chi_{\text{app}} \sin \varphi / 2$, D_L is a luminosity distance, the bulk plasma motion Lorentz factor is Γ , δ is the Doppler factor, and the observation angle $\varphi = \Gamma^{-1}$ (Cohen et al., 2007). The expression (8) has been obtained under the same assumption of synchrotron self-absorbed source, but the method utilizes the core shift effect — the shift of the observed radio core on different frequencies. This shift is due to the fact that the surface of optical depth $\tau = 1$ is situated at different distance from the central source for each frequency. We must stress that the relation (7) uses only the synchrotron self-absorbed source model, but the position of the radio core in the model is not known. If we use the core shift effect, we may also obtain the core position (Nokhrina, 2017):

$$\left(\frac{r_{\text{core}}}{\text{pc}} \right) = \frac{4.85}{\sin \varphi (1+z)^2} \left(\frac{\nu_{\text{obs}}}{\text{GHz}} \right)^{-1} \left(\frac{\eta_{\text{cs}}}{\text{mas GHz}} \right) \left(\frac{D_L}{\text{Gpc}} \right). \quad (10)$$

The relation for B_{cs} (8) has been obtained with more assumptions: equipartition between magnetic field energy and plasma energy assumption, and the Blanford-Königl model (Blanford and Königl, 1979) $B(r) = B_1(r_1/r)$, $n(r) = n_1(r_1/r)^2$, where n_1 and B_1 are particle number density and magnetic field magnitude at distance r along the jet equal to $r_1 = 1$ pc. Relation (8) provides the magnetic field amplitude together with its position along the jet.

Both expressions (7) and (8) are based on the model of uniform radiating sphere (Gould, 1979). In particular, such a model does not allow us to estimate the total magnetic flux, contained in a jet — one of the important values, defining the total jet power, and the value that could be restricted by the magnetically arrested disk model. Indeed, as the toroidal magnetic field B_φ dominates the major part of a jet, it is the toroidal component of a field we imply by the spectral flux measurement. However, it is the poloidal component B_P that carries the magnetic flux. However, the transversal modeling of field profiles allow us in a simple case of blazar jets, i.e. jets pointing almost directly at us, to calculate the flux from non-homogeneous cylindrical self-absorbed synchrotron source, and to correlate the measured magnetic field amplitude with the poloidal field in a jet that defines the total flux. Indeed, it has been shown by (Lyubarsky, 2009), that the relation

$$B_P = B_\varphi \frac{R_L}{r_\perp} \quad (11)$$

holds outside the light cylinder $R_L = c/\Omega_F$. Further we model the transversal magnetic field and particle number density profiles as follows. Inside the light cylinder the poloidal magnetic field remains almost constant (Beskin and Nokhrina, 2009), while $B_\varphi = B_0 r_\perp / R_L$. Both numerical and semi-analytical modeling (Nokhrina et al., 2015; Bromberg and Tchekhovskoy, 2016) show, that outside the light cylinder the power-law is a good approximation for magnetic field and particle number density profiles across the jet for small opening angles. We set

$$B_P = \begin{cases} B_0, & r_\perp \leq R_L, \\ B_0 \left(\frac{R_L}{r_\perp} \right)^2, & R_L < r_\perp \leq R_j, \end{cases} \quad (12)$$

$$B_{\varphi} = \begin{cases} B_0 \frac{r_{\perp}}{R_L}, & r_{\perp} \leq R_L, \\ B_0 \left(\frac{R_L}{r_{\perp}} \right), & R_L < r_{\perp} \leq R_j. \end{cases} \quad (13)$$

$$n = \begin{cases} n_0, & r_{\perp} \leq R_L, \\ n_0 \left(\frac{R_L}{r_{\perp}} \right)^2, & R_L < r_{\perp} \leq R_j, \end{cases} \quad (14)$$

where B_0 and n_0 are the magnetic field and particle number density amplitudes, i.e. magnitudes at the light cylinder R_L .

For the simplest case of a jet pointing almost at us, when the radiation domain may be treated as a stratified cylinder with the profiles (12)–(14), we calculate the spectral flux S_{ν} (see details in (Nokhrina, 2017)). Equating the obtained S_{ν} to the expression (6), we obtain the following relation for the amplitude magnetic field B_0 :

$$\left(\frac{B_0}{G} \right) = 6.4 \times 10^{-4} \frac{R_j}{R_L} \frac{\Gamma \delta}{1+z} \left(\frac{\nu_{\text{obs}}}{\text{GHz}} \right) \left(\frac{T_{\text{b, obs}}}{10^{12} \text{ K}} \right)^{-2}. \quad (15)$$

Here the fast rotation $\Gamma R_L \ll R_j$ is assumed. While R_j can be estimated through observations, the light cylinder radius is usually unknown. However, its value can be somewhat restricted by theoretical models predicting that Blandford-Znajek process works effectively for R_L of the order of $2r_g$ (Blandford and Znajek, 1977; Tchekhovskoy et al., 2012). Still, the value B_0 cannot be readily extracted from the observations.

The total flux Ψ in a jet with given cross-section magnetic field profile is defined as

$$\Psi = 2\pi \int_0^{R_j} B_P r_{\perp} dr_{\perp}. \quad (16)$$

Using the magnetic field profile (12) we obtain

$$\Psi = \pi B_0 R_L^2 \left(1 + 2 \ln \frac{R_j}{R_L} \right). \quad (17)$$

Substituting explicitly $B_0 R_L$ into (17) and using the correlation $B_0 R_L = 0.86 B_{\text{uni}} R_j$ following from (7) and (15), we obtain the relation for the magnetic flux:

$$\Psi = 2.7 B_{\text{uni, cs}} R_j \frac{r_g}{a} \left[1 + 2 \ln \frac{R_j a}{r_g} \right] = \frac{\Psi_a}{a}. \quad (18)$$

Here one may use B_{cs} or B_{uni} , since both values are obtained under the same assumptions on the geometry and structure of radiating domain. The amplitude magnetic flux $\Psi_a = a\Psi$. The equation (18) coincides with the expression for the magnetic flux in (Zamaninasab et al., 2014). The expression (18) for the flux depends inversely on a rotation rate a , because the dependence on the physical values in square brackets is logarithmically weak and can be neglected. Taking the fiducial value for $R_j/r_g \sim 10^3$, we take the expression in square brackets being of the order of a few to ten.

3 THE JET POWER AND THE ROTATION RATE

We apply the obtained expression for the flux (18) to test it against the following theoretical predictions. If we assume that most of the sources are in MAD state, we can compare the amplitude flux Ψ_a and Ψ_{MAD} and obtain the rotation parameter $a = \Psi_a/\Psi_{\text{MAD}}$. However, we must bear in mind that the energy losses mechanism Blanford and Znajek (1977) works effectively for relatively high rotation rates $a > 0.5$. Thus, with the difference in Ψ_{MAD} and Ψ_a is greater, we might think that the source is not in the MAD state.

We also use the obtained flux (18) to calculate the total jet power given by the equation (1). As the expression (1) depends on the product $\Psi a = \Psi_a$ (18) that depends on a logarithmically weakly only through the term $1 + 2 \ln(R_j a/r_g)$, so does the total power. So this result is independent on the assumption of the particular value for a . That is why such a test may be important for the flux determination. We do it for the magnetic field estimated by two methods: the brightness temperature measurements and the core shift measurements in order to compare the two methods.

We have found 48 sources meeting the following conditions: i. the observational angle of a jet must be small enough for the model of head-on jet for B_{uni} can be applied; ii. the source has a measured core shift, central black hole mass, and the apparent opening angle. We use the following samples: we take the brightness temperature measured by Kovalev et al. (2005) and the core shifts by Pushkarev et al. (2012). The apparent velocity β_{app} we take from (Lister et al., 2009). We also use the black hole masses M_{BH} and the accretion luminosities L_{acc} collected by Zamaninasab et al. (2014). For the unknown Lorentz factor we use $\Gamma = \sigma_M$, and the Michel's magnetization parameter σ_M has been evaluated by Nokhrina et al. (2015). We use for the observed opening angle the results from Pushkarev et al. (2009). This is in contrast with (Zamaninasab et al., 2014), where the causal connectivity across the jet $\Gamma\chi \sim 1$ is assumed. We obtain the magnetic field magnitudes using the above values and equations (7) and (8). On average, the values of B_{uni} is less and more scattered than values of B_{cs} , which is in agreement with results obtained in (Zdziarski et al., 2015). To calculate the flux using B_{cs} we employ $R_j = \chi \times 1 \text{ pc}$. For B_{uni} we use equation (10), so we define $R_j = r_{\text{core}}\chi$.

One of the possible upper limits on the magnetic field amplitude in relativistic jets may be imposed by MAD model. Magnetically arrested disk is a disk in a state of equilibrium of the accretion rate and the pressure of magnetic field frozen in previously accreted matter (Narayan et al., 2003; Tchekhovskoy et al., 2011; McKinney et al., 2012). There is observational support of AGNs staying in MAD state (Zamaninasab et al., 2014). Equation (18) relate the total magnetic flux in a jet with the observable jet radius, magnetic field, gravitational radius (through the black hole mass estimates), and unknown rotation rate a . Setting Ψ_{MAD} as the upper limit on a magnetic flux, one can obtain the lower limit for the rotational rate of a central black hole. Here we compare the magnetic flux Ψ calculated with expression (18) for B_{uni} , obtained by the brightness temperature measurements, or B_{cs} obtained by core shift measurements, and the magnetic flux Ψ_{MAD} set by MAD model. In order to obtain the magnetic flux predicted by MAD Ψ_{MAD} , we use the equation (Zamaninasab et al., 2014)

$$\Psi_{\text{MAD}} \approx 50 \sqrt{\dot{M} r_g^2 c}, \quad (19)$$

where we use relation between disk luminosity $L_{\text{acc}} = \eta \dot{M} c^2$.

The results for Ψ calculated for $a = 0.5$ and Ψ_{MAD} are presented in Table 1. We present in the table the values for Ψ_{MAD} (Zamaninasab et al., 2014), the total magnetic flux obtained using brightness temperature measurements Ψ_{br} and core shift measurements Ψ_{cs} . We see the reasonable agreement

between Ψ_{br} and Ψ_{cs} , although the former is more scattered. We see that $a\Psi \ll \Psi_{\text{MAD}}$ for almost all the sources for magnetic field estimates by both methods. If we assume that all the sources are in MAD state, the rotational rate of a black hole must be in a range (0.0001; 0.1) for 36 sources. Only 12 have the rotational rate between 0.1 and 1. Thus, assumption of the sources being in the MAD state leads us to a conclusion that the rotation must be much less than the critical one.

Otherwise, we may assume that 36 sources have rotation parameters close to critical $a \in [0.5; 1]$, but not in a MAD state. We must stress that the expressions for the magnetic field estimate through the core shift measurement are different here from the one used in (Zamaninasab et al., 2014). In this paper the Eq. (8) uses the assumptions from (Nokhrina et al., 2015) of the total outflow magnetization equal to the unity. This condition means that the total Poynting flux in a core region is equal to the total bulk particle kinetic energy flux, with about 1% (Sironi et al., 2013) of radiating particles having the relativistic energy distribution (2). This assumption has been used to estimate maximal possible Lorentz factor of the flow (Nokhrina et al., 2015), which correlates very good with the Lorentz factor estimates basing the observed super-luminal velocities (Lister et al., 2009). In this point our approach differs from the one used by (Zamaninasab et al., 2014).

In order to check our flux estimates, we test it against the total jet power (1). This result is robust under the model assumptions, since the total power depends on a very weakly. The calculation of the total jet power for the obtained flux is in Table 1. We compare the total power P_Ψ , calculated substituting (18) into (1), with the jet power, estimated basing on the correlation of P_{jet} with the luminosities of jet radio band Cavagnolo et al. (2010):

$$\left(\frac{P_{\text{jet}}}{10^{43} \text{ erg s}^{-1}} \right) = 3.5 \left(\frac{P_{200-400}}{10^{40} \text{ erg s}^{-1}} \right)^{0.64}. \quad (20)$$

We plot P_Ψ against the obtained with (20) power P_{jet} in Fig. 1. We observe the reasonable correlation of P_Ψ and P_{jet} . The histogram of the ratio of P_Ψ/P_{jet} is presented in Fig. 2. We see that the ratio has a well determined peak around a few. Although it gives the systematic excess of P_Ψ over P_{jet} , we state that P_Ψ is in accordance with P_{jet} bearing in mind uncertainties in the determination of all the values including P_{tot} . The systematic excess may be attributed to the probable overestimating the magnetic field B_{cs} , the hints of which we see in discrepancy between B_{cs} and B_{br} , the latter being lower.

We have also tested the jet power obtained with the flux determined by B_{uni} (see Fig. 1). The second method provides systematically lower powers and more scattering. This is in agreement with the result by (Zdziarski et al., 2015) who have found the scattering in magnetic field amplitude calculated with no equipartition assumption while still have the majority of sources having the equipartition magnetic field.

4 SUMMARY

We have discussed estimates for the magnetic flux using the jet core magnetic field obtained through the brightness temperature measurements and by the core shift effect. Usually, any estimates of the magnetic field in a radiating domain of relativistic jet cannot be readily put into the expression for the magnetic flux. This is because theoretical modeling show, that the toroidal magnetic field dominates the poloidal magnetic field outside the light cylinder. Thus, the field we measure using synchrotron self-Compton model of radiation, must be toroidal, while the magnetic flux is determined by the poloidal one. Consideration of transversal field configuration is needed to estimate accurately the magnetic flux in a jet using the available evaluation of magnetic field magnitude through observations — either using the

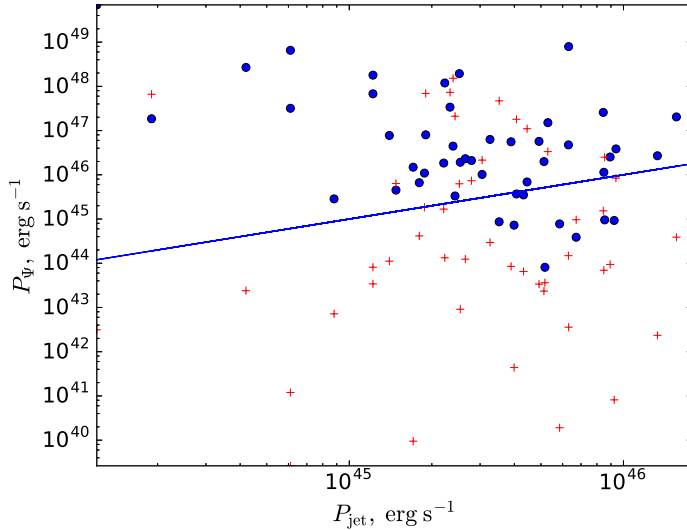


Figure 1. The jet power P_Ψ , calculated using magnetic flux, against the total kinetic jet power. The straight line is a theoretical prediction. The blue circles stand for the total flux obtained using the core shift effect, the red crosses are for the total flux obtained using the brightness temperature. The sources with the flux approximately equal to the MAD flux are in the upper left corner.

core-shift effect, or spectral flux measurements. In this work has been considered the simplest case — the transversal structure of jets observed with very small viewing angle.

We test the method of estimating the flux against the limiting flux determined by the magnetically arrested disk model. For 36 of 48 sources the obtained flux is much less than the MAD flux. This suggests either the extremely slow rotation rate $a \in (0.0001; 0.1)$ or that the sources are not in MAD state. For 12 sources both fluxes coincide for $a \in (0.1; 1)$ — the fast rotation that is needed for the efficient energy extraction from a black hole.

We also test the flux estimate against the total jet power determined by the electromagnetic mechanism of energy extraction. This result does not depend on the particular value for a , as the expression (1) depends on the product of Ψ and $a \Psi_a$ that can be estimated directly. In this case we see a good agreement between the total power determined by the flux and the total power obtained from the observations, with the distribution of powers ratio being well peaked around a few.

AUTHOR CONTRIBUTIONS

The results presented in the paper have been obtained by EN.

FUNDING

This work was supported by Russian Science Foundation, grant 16-12-10051.

ACKNOWLEDGMENTS

The author thanks the anonymous referees for the suggestions which helped to improve the paper. This research has made use of data from the MOJAVE database that is maintained by the MOJAVE team (Lister et al., 2009).

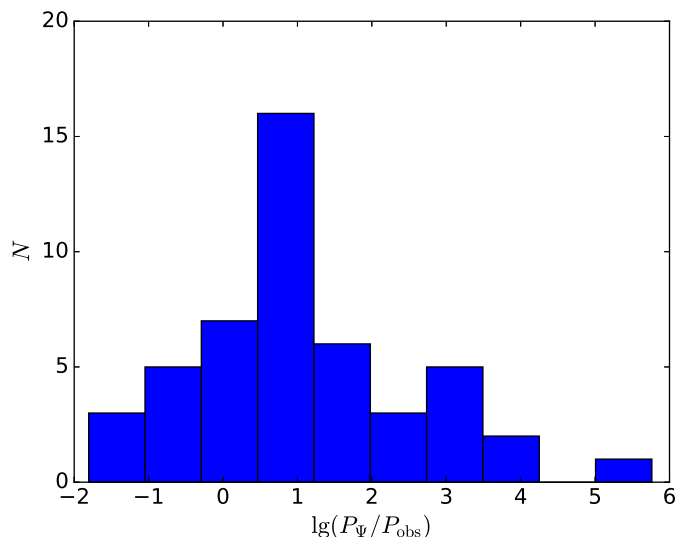


Figure 2. The histogram showing the number of sources with the ratio of calculated power P_Ψ to the total jet power P_{jet} , the ratio is in the log-scale. We see the systematic excess of power estimated through the flux against the jet power by a factor of few.

REFERENCES

- Abdo, A., Ackermann, M., Ajello, M., Baldini, L., Ballet, J., Barbiellini, G., et al. (2011). Fermi large area telescope observations of markarian 421: The missing piece of its spectral energy distribution. *Astrophysical Journal* 736, 131
- Beskin, V. (2010). Magnetohydrodynamic models of astrophysical jets. *Physics Uspekhi* 53, 1199–1233. doi:10.3367/UFNe.0180.201012b.1241
- Beskin, V. and Nokhrina, E. (2009). On the central core in mhd winds and jets. *Monthly Notices of Royal Astronomical Society* 397, 1486–1497. doi:10.1111/j.1365-2966.2009.14964.x
- Blanford, R. and Königl, A. (1979). Relativistic jets as compact radio sources. *Astrophysical Journal* 232, 34–48. doi:10.1086/157262
- Blanford, R. and Znajek, R. (1977). Electromagnetic extraction of energy from kerr black holes. *Monthly Notices of the Royal Astronomical Society* 179, 433–456. doi:10.1093/mnras/179.3.433
- Bromberg, O. and Tchekhovskoy, A. (2016). Relativistic mhd simulations of core-collapse grb jets: 3d instabilities and magnetic dissipation. *Monthly Notices of Royal Astronomical Society* 456, 1739–1760. doi:10.1093/mnras/stv2591
- Cavagnolo, K., McNamara, B., Nulsen, P., Carilli, C., Jones, C., and Bîrzan, L. (2010). A relationship between agn jet power and radio power. *Astrophysical Journal* 720, 1066–1072. doi:10.1088/0004-637X/720/2/1066
- Cohen, M., Lister, M., Homan, D., Kadler, M., Kellermann, K., Kovalev, Y., et al. (2007). Relativistic beaming and the intrinsic properties of extragalactic radio jets. *Astrophysical Journal* 658, 232–244. doi:10.1086/511063
- Gould, R. (1979). Compton and synchrotron processes in spherically-symmetric non-thermal sources. *Astronomy & Astrophysics* 76, 306–311
- Hiroani, K. (2005). Kinetic luminosity and composition of active galactic nuclei jets. *The Astrophysical Journal* 619, 73–85. doi:10.1086/426497

- Kovalev, Y., Kellermann, K., Lister, M., Homan, D., Vermeulen, R., Cohen, M., et al. (2005). Submilliarcsecond imaging of quasars and active galactic nuclei. iv. fine-scale structure. *The Astronomical Journal* 130, 2473–2505. doi:10.1086/497430
- Lister, M., Aller, H., Aller, M., Cohen, M., Homan, D., Kadler, M., et al. (2009). Mojave: Monitoring of jets in active galactic nuclei with vlba experiments. v. multi-epoch vlba images. *The Astronomical Journal* 137, 3718–3729. doi:10.1088/0004-6256/137/3/3718
- Lister, M., Aller, M., Aller, H., Homan, D., Kellermann, K., Kovalev, Y., et al. (2013). Mojave. x. parsec-scale jet orientation variations and superluminal motion in active galactic nuclei. *The Astronomical Journal* 146, 120–142. doi:10.1088/0004-6256/146/5/120
- Lobanov, A. (1998). Ultracompact jets in active galactic nuclei. *Astronomy & Astrophysics* 330, 79–89
- Lyubarsky, Y. (2009). Asymptotic structure of poynting-dominated jets. *The Astrophysical Journal* 698, 1570–1589. doi:10.1088/0004-637X/698/2/1570
- McKinney, J., Tchekhovskoy, A., and Blandford, R. (2012). General relativistic magnetohydrodynamic simulations of magnetically choked accretion flows around black holes. *Monthly Notices of the Royal Astronomical Society* 423, 3083–3117. doi:10.1111/j.1365-2966.2012.21074.x
- Narayan, R., Igumenshchev, I., and Abramowicz, M. (2003). Magnetically arrested disk: an energetically efficient accretion flow. *Publications of the Astronomical Society of Japan* 55, L69–L72. doi:10.1093/pasj/55.6.L69
- Nokhrina, E. (2017). Brightness temperature - obtaining the physical properties of a non-equipartition plasma. *Monthly Notices of Royal Astronomical Society* 468, 2372–2381. doi:10.1093/mnras/stx521
- Nokhrina, E., Beskin, V., Kovalev, Y., and Zheltoukhov, A. (2015). Intrinsic physical conditions and structure of relativistic jets in active galactic nuclei. *Monthly Notices of Royal Astronomical Society* 447, 2726–2737. doi:10.1093/mnras/stu2587
- O’Sullivan, S. and Gabuzda, D. (2009). Magnetic field strength and spectral distribution of six parsec-scale active galactic nuclei jets. *Monthly Notices of Royal Astronomical Society* 400, 26–42. doi:10.1111/j.1365-2966.2009.15428.x
- Pushkarev, A., Hovatta, T., Kovalev, Y., Lister, M., Lobanov, A., Savolainen, T., et al. (2012). Mojave: Monitoring of jets in active galactic nuclei with vlba experiments. ix. nuclear opacity. *Astronomy & Astrophysics* 545, A113. doi:10.1051/0004-6361/201219173
- Pushkarev, A., Kovalev, Y., Lister, M., and Savolainen, T. (2009). Jet opening angles and gamma-ray brightness of agn. *Astronomy & Astrophysics* 507, L33–L36. doi:10.1051/0004-6361/200913422
- Sironi, L., Spitkovsky, A., and Arons, J. (2013). The maximum energy of accelerated particles in relativistic collisionless shocks. *The Astrophysical Journal* 771, 54. doi:10.1088/0004-637X/771/1/54
- Tchekhovskoy, A., McKinney, J., and Narayan, R. (2012). General relativistic modeling of magnetized jets from accreting black holes. *Journal of Physics: Conference Series* 372. doi:10.1088/1742-6596/372/1/012040
- Tchekhovskoy, A., Narayan, R., and McKinney, J. (2011). Efficient generation of jets from magnetically arrested accretion on a rapidly spinning black hole. *Monthly Notices of the Royal Astronomical Society* 418, L79–L83. doi:10.1111/j.1745-3933.2011.01147.x
- Zamaninasab, M., Clausen-Brown, E., Savolainen, T., and Tchekhovskoy, A. (2014). Dynamically important magnetic fields near accreting supermassive black holes. *Nature* 510, 126–128. doi:10.1038/nature13399
- Zdziarski, A., Sikora, M., Pjanka, P., and Tchekhovskoy, A. (2015). Core shifts, magnetic fields and magnetization of extragalactic jets. *Monthly Notices of Royal Astronomical Society* 451, 927–935. doi:10.1093/mnras/stv986

Table 1. Jet important observed and derived parameters.

Source	z	Ψ_{MAD} G cm ²	Ψ_{br} G cm ²	Ψ_{cs} G cm ²	P_{Ψ} [erg s ⁻¹]	P_{jet} [erg s ⁻¹]
(1)	(2)	(3)	(4)	(5)	(6)	(7)
0133+476	0.859	5.51×10^{33}	1.17×10^{31}	5.34×10^{32}	1.92×10^{46}	2.54×10^{45}
0212+735	2.367	5.77×10^{35}	5.97×10^{32}	8.93×10^{32}	8.10×10^{43}	5.17×10^{45}
0234+285	1.206	5.71×10^{34}	1.24×10^{34}	5.31×10^{32}	8.65×10^{44}	3.52×10^{45}
0333+321	1.259	9.36×10^{34}	6.00×10^{32}	3.81×10^{32}	3.88×10^{44}	6.72×10^{45}
0336-019	0.852	1.55×10^{34}	1.45×10^{32}	2.12×10^{33}	6.31×10^{46}	3.26×10^{45}
0403-132	0.571	3.00×10^{34}	4.34×10^{33}	1.09×10^{33}	6.89×10^{45}	4.45×10^{45}
0528+134	2.070	6.05×10^{34}	1.61×10^{30}	3.24×10^{32}	7.75×10^{44}	5.85×10^{45}
0605-085	0.870	1.68×10^{34}	9.94×10^{33}	1.70×10^{33}	4.45×10^{46}	2.39×10^{45}
0736+017	0.189	6.94×10^{32}	3.86×10^{30}	1.29×10^{33}	2.68×10^{48}	4.20×10^{44}
0738+313	0.631	1.48×10^{35}	3.22×10^{33}	2.71×10^{33}	4.51×10^{45}	1.48×10^{45}
0748+126	0.889	4.33×10^{34}	1.39×10^{32}	1.90×10^{33}	2.31×10^{46}	2.65×10^{45}
0827+243	0.943	1.81×10^{34}	1.72×10^{32}	6.87×10^{32}	6.62×10^{45}	1.80×10^{45}
0836+710	2.218	1.78×10^{35}	7.19×10^{31}	8.30×10^{32}	1.11×10^{45}	1.78×10^{46}
0906+015	1.026	9.81×10^{33}	5.66×10^{32}	3.90×10^{32}	1.02×10^{46}	3.05×10^{45}
0917+624	1.453	2.25×10^{34}	3.93×10^{33}	5.62×10^{32}	3.68×10^{45}	4.07×10^{45}
0945+408	1.249	2.27×10^{34}	1.29×10^{32}	2.32×10^{33}	4.75×10^{46}	6.30×10^{45}
1038+064	1.265	4.33×10^{34}	1.16×10^{32}	8.49×10^{32}	3.51×10^{45}	4.32×10^{45}
1127-127	1.184	7.44×10^{34}	2.10×10^{32}	3.45×10^{33}	2.53×10^{46}	8.94×10^{45}
1156+295	0.725	6.33×10^{33}	3.48×10^{31}	8.91×10^{32}	5.58×10^{46}	3.89×10^{45}
1219+285	0.103	2.83×10^{32}	4.34×10^{33}	2.29×10^{33}	1.85×10^{47}	1.90×10^{44}
1222+216	0.434	1.50×10^{34}	6.71×10^{33}	2.28×10^{33}	8.01×10^{46}	1.90×10^{45}
1253-055	0.536	2.76×10^{33}	3.93×10^{30}	5.84×10^{33}	7.93×10^{48}	6.31×10^{45}
1308+326	0.997	1.11×10^{34}	4.89×10^{32}	8.28×10^{32}	2.10×10^{46}	2.79×10^{45}
1334-127	0.539	1.28×10^{33}	1.01×10^{29}	1.27×10^{32}	1.49×10^{46}	1.71×10^{45}
1458+718	0.904	5.84×10^{34}	2.83×10^{31}	3.03×10^{33}	2.70×10^{46}	1.33×10^{46}
1502+106	1.839	2.17×10^{34}	3.48×10^{31}	1.43×10^{33}	5.70×10^{46}	4.92×10^{45}
1510-089	0.360	2.30×10^{33}	1.01×10^{31}	1.42×10^{33}	6.79×10^{47}	1.22×10^{45}
1546+027	0.414	5.84×10^{33}	1.11×10^{30}	8.20×10^{33}	6.53×10^{48}	6.10×10^{44}
1606+106	1.232	2.44×10^{34}	1.86×10^{33}	3.95×10^{33}	1.51×10^{47}	5.30×10^{45}
1611+343	1.400	5.21×10^{34}	6.59×10^{32}	8.55×10^{33}	2.57×10^{47}	8.44×10^{45}
1633+382	1.813	4.53×10^{34}	1.20×10^{32}	1.53×10^{33}	1.14×10^{46}	8.48×10^{45}
1637+574	0.751	5.51×10^{34}	7.76×10^{32}	1.89×10^{33}	1.09×10^{46}	1.88×10^{45}
1641+399	0.593	5.64×10^{34}	9.82×10^{31}	2.86×10^{33}	1.99×10^{46}	5.13×10^{45}
1655+077	0.621	1.65×10^{32}	1.77×10^{32}	1.21×10^{32}	3.39×10^{47}	2.33×10^{45}
1749+096	0.322	7.70×10^{33}	3.28×10^{29}	3.62×10^{33}	3.19×10^{47}	6.10×10^{44}
1803+784	0.680	1.11×10^{33}	1.04×10^{31}	9.88×10^{32}	1.19×10^{48}	2.23×10^{45}
1823+568	0.664	7.61×10^{32}	7.49×10^{31}	1.32×10^{33}	1.93×10^{48}	2.52×10^{45}
1828+487	0.692	5.21×10^{33}	5.52×10^{31}	1.26×10^{33}	2.04×10^{47}	1.56×10^{46}
1849+670	0.657	1.14×10^{34}	6.34×10^{31}	9.40×10^{33}	1.79×10^{48}	1.22×10^{45}
1928+738	0.302	5.27×10^{33}	2.58×10^{31}	6.78×10^{32}	7.75×10^{46}	1.40×10^{45}
2121+053	1.941	3.10×10^{34}	4.34×10^{30}	1.77×10^{32}	7.27×10^{44}	3.99×10^{45}
2155-152	0.672	3.64×10^{32}	1.94×10^{32}	2.44×10^{31}	3.32×10^{45}	2.43×10^{45}

2200+420	0.069	9.05×10^{32}	3.27×10^{30}	1.54×10^{34}	6.95×10^{49}	1.20×10^{44}
2201+315	0.295	2.61×10^{34}	2.54×10^{31}	5.06×10^{32}	2.85×10^{45}	8.80×10^{44}
2230+114	1.037	2.27×10^{34}	2.64×10^{30}	2.82×10^{32}	9.27×10^{44}	9.25×10^{45}
2251+158	0.859	1.81×10^{34}	4.89×10^{32}	1.05×10^{33}	3.85×10^{46}	9.39×10^{45}
2345-167	0.576	3.36×10^{33}	1.32×10^{32}	4.36×10^{32}	1.84×10^{46}	2.21×10^{45}
2351+456	1.986	5.84×10^{34}	3.36×10^{33}	6.56×10^{32}	9.56×10^{44}	8.54×10^{45}

Notes. Columns are as follows: (1) source name (B1950); (2) redshift z as collected by (Lister et al., 2013); (3) the MAD magnetic flux obtained using Equation (19); (4) derived total magnetic flux using the brightness temperature measurements; (5) derived total magnetic flux using the core shift measurements; (6) The jet power estimate using the magnetic field B_{cs} ; (7) the total jet power estimated using the correlation between the jet power and radio flux (Cavagnolo et al., 2010), collected from (Nokhrina et al., 2015).